



## Original Article

Structural and mechanical properties of microwave sintered Al–Ni<sub>50</sub>Ti<sub>50</sub> compositesM. Penchal Reddy <sup>a</sup>, F. Ubaid <sup>a</sup>, R.A. Shakoor <sup>a,\*</sup>, A.M.A. Mohamed <sup>b</sup>, W. Madhuri <sup>c</sup><sup>a</sup> Center for Advanced Materials, Qatar University, Doha 2713, Qatar<sup>b</sup> Department of Metallurgical and Materials Engineering, Suez University, Suez 43721, Egypt<sup>c</sup> School of Advanced Sciences, VIT University, Vellore 632 014, India

## ARTICLE INFO

## Article history:

Received 29 June 2016

Received in revised form

20 July 2016

Accepted 21 July 2016

Available online 26 July 2016

## Keywords:

Aluminum

Mechanical alloying

Ni<sub>50</sub>Ti<sub>50</sub> amorphous reinforcement

Microwave processing

Mechanical properties

## ABSTRACT

Metal matrix composites (MMCs) have become attractive for structural engineering applications due to their excellent specific strength and are becoming an alternative to the conventional materials particularly in the automotive, aerospace and defence industries. The present work aims to synthesize and characterize the Al–Ni<sub>50</sub>Ti<sub>50</sub> composites using microwave sintering technique with various weight fractions of reinforced particles. Ni-based metallic glass (Ni<sub>50</sub>Ti<sub>50</sub>) powders were prepared by mechanical alloying. The microstructure and mechanical properties of Al–Ni<sub>50</sub>Ti<sub>50</sub> composites were examined by X-ray diffraction (XRD), scanning electron microscopy (SEM), Vickers hardness and compression testing. The results show that the maximum average hardness value of  $116 \pm 5$  Hv was measured for Al–20 wt% Ni<sub>50</sub>Ti<sub>50</sub> composite. The average compression strength of the composites was increased by 211% compared to pure Al.

© 2016 The Authors. Publishing services by Elsevier B.V. on behalf of Vietnam National University, Hanoi.

This is an open access article under the CC BY license (<http://creativecommons.org/licenses/by/4.0/>).

## 1. Introduction

Particulate reinforced metal matrix composites (MMCs) have been widely used in aerospace and automobile industries due to their promising properties such as low cost, light weight, ease of fabrication, enhanced mechanical properties at high temperature and higher strength to weight ratios [1–6]. Generally, ceramic particles such as SiC, Al<sub>2</sub>O<sub>3</sub> and B<sub>4</sub>C having high strength, high elastic modulus, wear and fatigue resistance are incorporated in Aluminum matrix to fabricate particulate composites [7–9]. However, the major problems in synthesizing aluminum metal matrix composites (AMMCs) are the reduced ductility, inhomogeneous distribution of the reinforcements residual porosity at the interface and formation of brittle phases resulting from chemical reactions during fabrication process [10]. Due to these disadvantages the use of MMCs has been restricted in many applications. It is widely recognized that the mechanical properties of MMCs can be controlled by the size and volume fraction of the reinforcements as well as the nature of the matrix reinforcements interface bonding strength [1].

One of the methods to overcome these problems is to reinforce the matrix with alternative reinforcements that not only possess the advantages of ceramic reinforcements but can also overcome the existing drawbacks. In this context, metallic amorphous alloys or bulk metallic glasses are a promising option. Metallic glasses have been recently proposed as a novel type of reinforcement in metal matrix composites, able to overcome the disadvantages of conventional ceramic reinforcing particles [11–16].

Aluminum metal matrix composites are one of the most demanding engineering materials in the category of metal matrix composites (MMCs) due to the combination of their light weight and excellent mechanical and tribological properties. These composites have been widely used for structural and functional applications in automotive and aerospace industries [17–19]. The optimum properties of AMMCs depend on good selection of the reinforcing particles and the processing technique/parameters.

In the recent years, some modern processing techniques have been in use to sinter Al-based composites such as laser [20], spark plasma and microwave sintering [21–24]. In case of Al-MMCs synthesized by microwave sintering it offers many advantages [25]. It is a rapid sintering technique which employs two directional heating through a combined action of microwaves and microwave coupled external heating source. By using microwave sintering technique, the melting temperatures of light metals like Al, Mg can be achieved in a relatively shorter period of time. Because of the accelerated

\* Corresponding author.

E-mail address: [shakoor@qu.edu.qa](mailto:shakoor@qu.edu.qa) (R.A. Shakoor).

Peer review under responsibility of Vietnam National University, Hanoi.

heating rates, the resulting products have controlled grain growth, uniform microstructure and higher density. Therefore, the concurrent use of time and energy saving makes microwave sintering a better technique to produce fine composite products.

A study of available open literature shows that the investigations on amorphous alloys incorporation in Al-matrices are still in the early stage and as only limited studies have been successfully carried out so far [22,26,27]. In this work, Ni<sub>50</sub>Ti<sub>50</sub> amorphous alloys powders synthesized via milling process were incorporated into pure Al matrix using the blend-press-sintering process. The structure and mechanical properties of the microwave sintered Al-composites were also investigated.

## 2. Experimental procedures

### 2.1. Materials

Aluminum (99.5% purity, 7–10 μm average particle size), nickel (99.5% purity, 145 μm average particle size) and titanium (99.5% purity, 110 μm average particle size) powders were purchased from Alfa Aesar, were used as starting materials in this study.

### 2.2. Preparation of amorphous reinforcements

Amorphous powder with composition Ni<sub>50</sub>Ti<sub>50</sub> (at.%) were first ball-milled using a Retsch PM 200 planetary ball mill for 55 h. The ball to powder ratio was maintained at 5:1. The balls and vials are made of tungsten carbide. The rotating speed of the vial was

maintained at 300 rpm. The structural analysis of the amorphous powder was conducted using X-ray diffraction and scanning electron microscope.

### 2.3. Preparation of Al-composites

To produce Al composites, elemental Al powder was mixed with different weight fractions of Ni<sub>50</sub>Ti<sub>50</sub> amorphous powder (5, 10, 15 and 20 wt%) as the test materials with the chemical compositions shown in Table 1. All the mixed powders were placed in planetary ball mill at 200 rpm for 1hr. No balls were used in this stage. The blended powders (~2.0 g) were then compacted into cylindrical pellets by applying uniaxial pressure of 10 MPa. The compacted pellets were then sintered at 550 °C for 30 min. The entire synthesis process is schematically represented by the flowchart in Fig. 1.

Microwave sintering was carried out in a microwave furnace with a silicon carbide ceramic crucible and alumina insulation in it (VB Ceramic Consultants, Chennai, India). The green samples were placed in the center of the cavity and sintered in a microwave furnace (multimode cavity) at 2.45 GHz. SiC was selected as a microwave susceptor to assist heating and sintering of the green samples. The sintering temperature was set at 550 °C ± 5 °C with a holding time of 30 min and an approximate heating rate of 25 °C/min. The sintered samples were then slowly cooled down to room temperature. The temperature was measured using infrared pyrometer.

### 2.4. Characterization

The phase identification of the amorphous powders and prepared Al-composites was examined using a panalytical X'pert Pro diffractometer with CuKα radiation (λ = 0.15406 nm). The XRD patterns were recorded in the 2θ range of 30–90° with step size of 0.02° and a scanning rate of 1.5 degs./min. The microstructural characterization of the sintered composites were examined using scanning electron microscopy (SEM, Jeol Neoscope JSM 6000). The microhardness values of the samples, was measured using a Vicker

**Table 1**  
Chemical compositions of the starting powders in this study.

S. no.	Materials	Al (wt%)	Ni <sub>50</sub> Ti <sub>50</sub> (wt%)
1	Pure Al	100	00
2	Al-5wt%Ni <sub>50</sub> Ti <sub>50</sub>	95	5
3	Al-10wt%Ni <sub>50</sub> Ti <sub>50</sub>	90	10
4	Al-15wt%Ni <sub>50</sub> Ti <sub>50</sub>	85	15
5	Al-20wt%Ni <sub>50</sub> Ti <sub>50</sub>	80	20

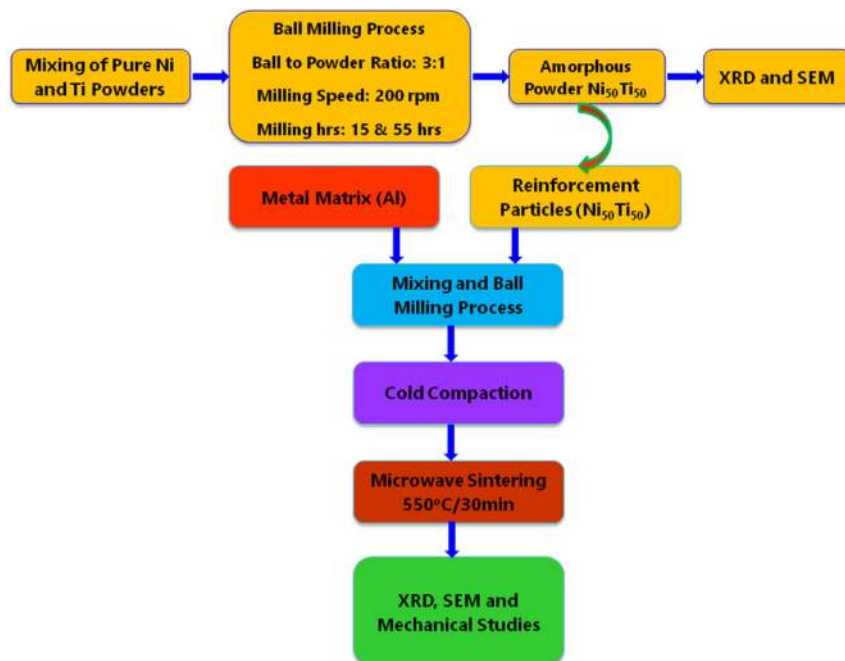


**Fig. 1.** Process flow chart for production of Al-composites.

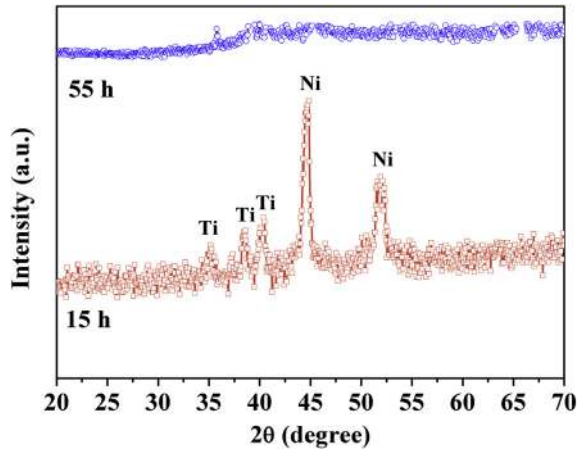


Fig. 2. XRD patterns of  $\text{Ni}_{50}\text{Ti}_{50}$  amorphous alloy powder at 15 h and 55 h.

microhardness Tester (MKV-h21, with applied load of 1 kgf for 15 s), are the average of at least five successive indentations for each sample. Universal testing machine-Lloyd 50 kN at a strain rate  $10^{-4}$ /sec was used to measure the compressive properties of the cylindrical samples with diameter of 10 mm and height of 3 mm.

### 3. Results and discussion

Fig. 2 shows the X-ray diffraction patterns of  $\text{Ni}_{50}\text{Ti}_{50}$  powders milled for various milling times (15 and 55 h). The characteristic elemental peaks of Ni and Ti peaks with high intensity observed in the raw materials were seen to gradually transform to amorphous halo. The diffused halo characteristics observed in the XRD pattern is typical of the amorphous structure which confirmed the amorphous state of the blended powders that was observed after 55 h [28] of milling.

The morphologies of the as-received Ni, Ti and ball milled  $\text{Ni}_{50}\text{Ti}_{50}$  powders are shown in Fig. 3 (a, b and c, respectively). The nickel powder (Fig. 3a) consists planar (with sharp corners) and irregular shaped particles ranging between 100 and 140  $\mu\text{m}$ . Fig. 3b shows spherical shaped Ti particles with average particle size of 30–100  $\mu\text{m}$ . Fig. 3c reveals that the ball-milled  $\text{Ni}_{50}\text{Ti}_{50}$  powder particles are mostly rounded and have regular size ranging between

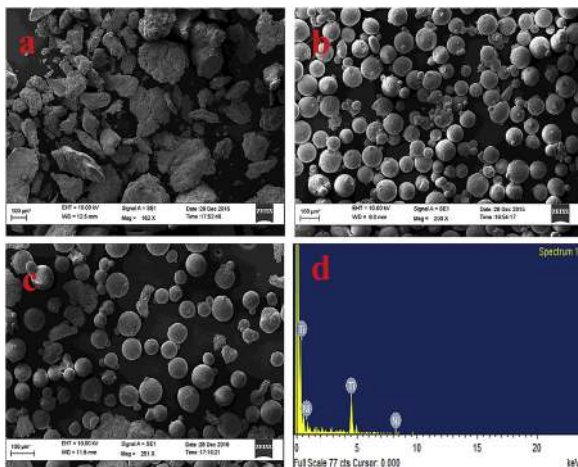


Fig. 3. The microstructural characteristics of the as-received Ni, Ti and the ball-milled  $\text{Ni}_{50}\text{Ti}_{50}$  powder (a–c). (d) Typical EDX spectra for  $\text{Ni}_{50}\text{Ti}_{50}$  amorphous powder.

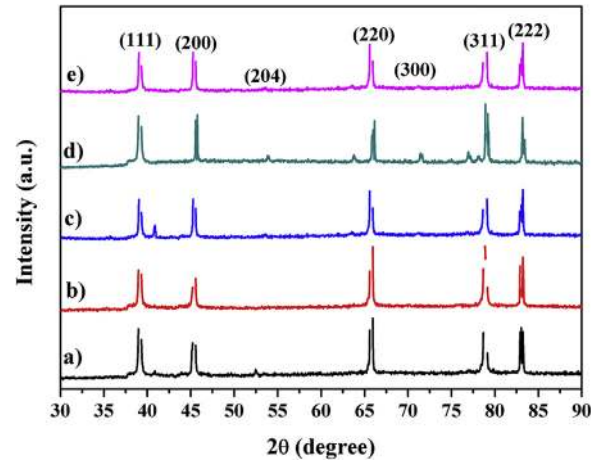


Fig. 4. XRD patterns of the microwave sintered (a) pure Al, (b) Al-5wt% $\text{Ni}_{50}\text{Ti}_{50}$ , (c) Al-10wt% $\text{Ni}_{50}\text{Ti}_{50}$  (d) Al-15wt% $\text{Ni}_{50}\text{Ti}_{50}$  and (e) Al-20wt% $\text{Ni}_{50}\text{Ti}_{50}$ .

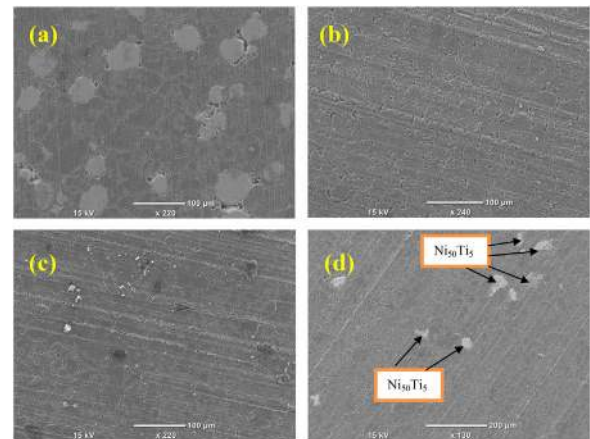


Fig. 5. SEM micrographs of (a) pure Al, (b) Al-10wt% $\text{Ni}_{50}\text{Ti}_{50}$  (c) Al-15wt% $\text{Ni}_{50}\text{Ti}_{50}$  and (d) Al-20wt% $\text{Ni}_{50}\text{Ti}_{50}$ .

70  $\mu\text{m}$  and 130  $\mu\text{m}$ , which is relatively lower than particle sizes of the as received Ni (149  $\mu\text{m}$ ) and Ti (110  $\mu\text{m}$ ) powders.

The phases identification of the microwave sintered pure Al and Al- $\text{Ni}_{50}\text{Ti}_{50}$  composites is shown in Fig. 4. It can be observed that all peaks corresponds to Al and  $\text{Ni}_{50}\text{Ti}_{50}$  phases due to shorter sintering time. Phase identification indicates the presence of f.c.c.–Al peaks, and absence of any secondary phase. The peaks at  $2\theta$  values of 38.971, 45.764, 65.594, 78.931 and 83.177 correspond to Al (JCPDS # 04-0787) with miller indices of (111), (200), (220), (300), (311) and (222), respectively.

Fig. 5 represents the microstructures of the Al-composites containing 5, 15 and 20% weight ratio of  $\text{Ni}_{50}\text{Ti}_{50}$ . Microstructural observations showed that the amorphous particles are distributed throughout the aluminum matrix and the primary aluminum matrix is indicated by the patches of rough matrix. The matrix phase is shown as dark phase, while the amorphous particles phase is white. Furthermore, no growth of particles was observed, particularly near their grain boundaries, at which the heat-affected zone is the greatest during the MWS process. It is clear from Fig. 5d that the fine microstructure with uniform distribution of reinforcement. It seems that the application of microwaves between aluminum particles accompanied by the removal of the surface oxides layer on the initial powder as advantage of microwave sintering lead to pore-free microstructure.

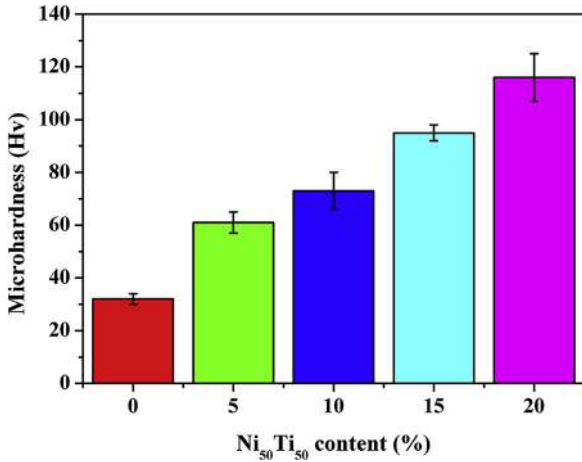


Fig. 6. Bar graph of microhardness of Al–Ni<sub>50</sub>Ti<sub>50</sub> composites as a function of Ni<sub>50</sub>Ti<sub>50</sub>.

An improvement in microhardness was observed in the aluminum matrix with the addition of Ni<sub>50</sub>Ti<sub>50</sub> amorphous particulates, as are shown in Fig. 6 and Table 2. The increase in microhardness of the aluminum metal matrix with the addition of Ni<sub>50</sub>Ti<sub>50</sub> reinforcements can be attributed primarily to the: (i) presence of harder amorphous powder reinforcement in the matrix and (ii) higher constraint to the localized matrix deformation due to the presence of harder phases. These results are consistent with the trend observed by other investigators [28].

In attempt to evaluate the mechanical properties of the composites, compression test was conducted at room temperature under uniaxial compressive loading and the stress–strain curves are shown in Fig. 7. Obviously, the compressive strength value of Al–Ni<sub>50</sub>Ti<sub>50</sub> composite is significantly higher than that of the pure

Table 2  
Mechanical properties of Ni<sub>50</sub>Ti<sub>50</sub> amorphous alloy particle reinforced Al-composites.

Materials	Microhardness (HV)	Compressive properties	
		0.2% CYS (MPa)	UCS (MPa)
Pure Al	32 ± 2	63 ± 2	243 ± 5
Al-5wt%Ni <sub>50</sub> Ti <sub>50</sub>	61 ± 3	83 ± 4	355 ± 3
Al-10wt%Ni <sub>50</sub> Ti <sub>50</sub>	73 ± 8	97 ± 7	415 ± 6
Al-15wt%Ni <sub>50</sub> Ti <sub>50</sub>	95 ± 1	115 ± 3	525 ± 8
Al-20wt%Ni <sub>50</sub> Ti <sub>50</sub>	116 ± 5	134 ± 9	589 ± 2

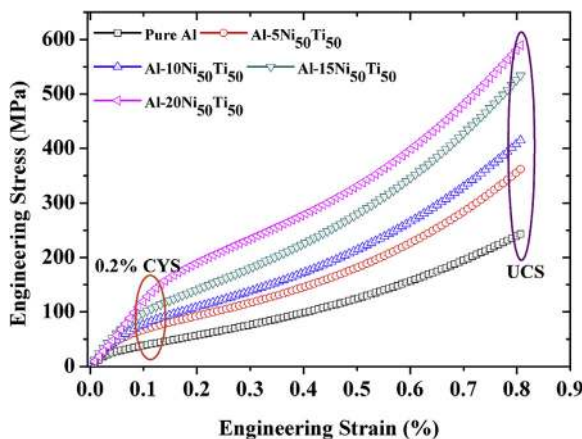


Fig. 7. Compression curves of the pure Al and composite materials.

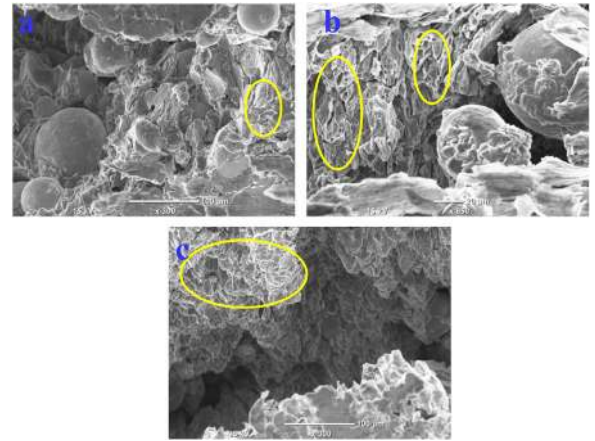


Fig. 8. The fracture morphology of (a) pure Al, (b) Al-10wt%Ni<sub>50</sub>Ti<sub>50</sub> and (c) Al-20wt%Ni<sub>50</sub>Ti<sub>50</sub>.

Al, suggesting that the Ni<sub>50</sub>Ti<sub>50</sub> particle can strongly enhance the mechanical strength of the Al matrix. Particular, Al-20 wt% Ni<sub>50</sub>Ti<sub>50</sub> composite exhibits high compressive yield strength about 134 ± 9 MPa.

The fractographic morphologies of the pure Al and its composites under compressive loading is presented in Fig. 8 (a–c). It is clearly showing shear mode fracture in both pure Al and its composites. It attributes to the compressive deformation of the developed Al-composites is considerably indifferent. We have noticed that the shear mode fractures were less in pure Al compared to its composites. The Al dimples on the Ni<sub>50</sub>Ti<sub>50</sub> surfaces (Fig. 8b) showed that a good interfacial bonding strength existed between the Ni<sub>50</sub>Ti<sub>50</sub> and the Al matrix. The Al dimples at their bottoms indicated that the bonding between the Ni and the Al matrix was in good condition. The fracture morphology of Al–Ni<sub>50</sub>Ti<sub>50</sub> composites produced by microwave sintering method is similar to that of the NiTi60/6061Al material produced by the friction stir processing created by Ni et al. [29].

#### 4. Conclusions

The Ni<sub>50</sub>Ti<sub>50</sub> metallic glass particles were prepared by ball milling. XRD investigations have revealed that the studied powders after 55 h of ball milling were amorphous. Ni<sub>50</sub>Ti<sub>50</sub> metallic glass particles reinforced Al-metal matrix composites were successfully synthesized by microwave sintering method. Microstructural characterization results showed the homogeneous distribution of amorphous particles with small porosity at some locations. The composite with 20% amorphous particle content exhibited the better microhardness (116 ± 5 Hv) and compressive yield strength (134 ± 9 MPa). Microwave heating can produce Al/Ni<sub>50</sub>Ti<sub>50</sub> composites by with saving energy and time.

#### Acknowledgment

This publication was made possible by NPRP Grant 7-159-2-076 from the Qatar National Research Fund (a member of the Qatar Foundation). Statements made herein are solely the responsibility of the authors.

#### References

[1] T.W. Clyne, P.J. Withers, *An Introduction to Metal Matrix Composites*, Cambridge University Press, Cambridge, 1993.

- [2] N. Chawla, Y.L. Shen, Mechanical behavior of particle reinforced metal matrix composites, *Adv. Eng. Mater.* 6 (2001) 357–370.
- [3] J.M. Torralba, C.E. da Costa, F. Velasco, P/M aluminum matrix composites: an overview, *J. Mater. Process. Technol.* 133 (2003) 203–206.
- [4] T. Christman, A. Needleman, S. Suresh, An experimental and numerical study of deformation in metal-ceramic composites, *Acta Metall.* 37 (1989) 3029–3050.
- [5] I.A. Ibrahim, F.A. Mohamed, E.J. Lavernia, Particulate reinforced metal matrix composites—a review, *J. Mater. Sci.* 26 (1991) 1137–1156.
- [6] T.W. Clyne, P.J. Withers, *An Introduction to Metal Matrix Composites*, Cambridge University Press, New York, 1999.
- [7] C. Yan, W. Lifeng, R. Jianyue, Multi-functional SiC/Al composites for aerospace applications, *Chin. J. Aeronaut.* 21 (2008) 578–584.
- [8] E. Ghasali, A. Pakseresht, F.S. Kooshail, M. Agheli, T. Ebadzadeh, Mechanical properties and microstructure characterization of spark plasma and conventional sintering of Al-SiC-TiC composites, *J. Alloy Cmpds* 666 (2016) 366–371.
- [9] D. Garbiec, M. Jurczyk, N.L. Zayonts, T. Mościcki, Properties of Al–Al<sub>2</sub>O<sub>3</sub> composites synthesized by spark plasma sintering method, *Arch. Civ. Mech. Eng.* 15 (2015) 933–939.
- [10] Z.W. Wang, M. Song, C. Sun, Y.H. He, Effects of particle size and distribution on the mechanical properties of SiC reinforced Al–Cu alloy composites, *Mater. Sci. Eng. A* 528 (2011) 1131–1137.
- [11] M.H. Lee, J.H. Kim, J.S. Park, J.C. Kim, W.T. Kim, D.H. Kim, Fabrication of Ni–Nb–Ta metallic glass reinforced Al-based alloy matrix composites by infiltration casting process, *Scr. Mater.* 50 (2004) 1367–1371.
- [12] P. Yu, K.B. Kim, J. Das, F. Baier, W. Xu, J. Eckert, Phase stability and its effect on the deformation behavior of Ti–Nb–Ta–In/Cr β alloys, *Scr. Mater.* 54 (2006) 1445–1450.
- [13] S. Scudino, K.B. Surreddi, S. Sager, M. Sakaliyska, J.S. Kim, W. Loser, J. Eckert, Production and mechanical properties of metallic glass-reinforced Al-based metal matrix composites, *J. Mater. Sci.* 43 (2008) 4518–4526.
- [14] S. Scudino, G. Liu, K.G. Prashanth, B. Bartusch, K.B. Surreddi, B.S. Murty, J. Eckert, Mechanical properties of Al-based metal matrix composites reinforced with Zr-based glassy particles produced by powder metallurgy, *Acta Mater.* 57 (2009) 2029–2039.
- [15] D.V. Dudina, K. Georganakakis, Y. Li, M. Aljerf, A. LeMoulec, A.R. Yavari, A. Inoue, A magnesium alloy matrix composite reinforced with metallic glass, *Comp. Sci. Technol.* 69 (2009) 2734–2736.
- [16] D.V. Dudina, K. Georganakakis, M. Aljerf, Y. Li, M. Braccini, A.R. Yavari, A. Inoue, Cu-based metallic glass particle additions to significantly improve overall compressive properties of an Al alloy, *Compos. Part A* 41 (2010) 1551–1557.
- [17] M.K. Surappa, Aluminum matrix composites: challenges and opportunities, *Sadhana* 28 (2003) 319–334.
- [18] A. Heinz, A. Haszler, C. Keidel, S. Moldenhauer, R. Benedictus, W.S. Miller, Recent development in aluminum alloys for aerospace applications, *Mater. Sci. Eng. A* 280 (2000) 102–107.
- [19] H.P. Degischer, Innovative light metals: metal matrix composites and foamed aluminium, *Mater. Des.* 18 (1997) 221–226.
- [20] S. Jain, K. Chandra, V. Agarwala, Microstructure and mechanical properties of vacuum hot pressed p/m short steel fiber reinforced aluminum matrix composites, *ISRN Mater. Sci.* 2014 (2014), 312908 (9 pages).
- [21] M. Gupta, W.L.E. Wong, Characteristics of aluminum and magnesium based nanocomposites processed using hybrid microwave sintering, *J. Microw. Power Electromagn. Energy* 44 (1) (2010) 14–27.
- [22] S. Jayalakhshmi, S. Gupta, S. Sankarayanan, S. Sahu, M. Gupta, Structural and mechanical properties of Ni<sub>60</sub>Nb<sub>40</sub> amorphous alloy particle reinforced Al-based composites produced by microwave-assisted rapid sintering, *Mater. Sci. Eng. A* 581 (2013) 119–127.
- [23] E. Ghasali, M. Alizadeh, T. Ebadzadeh, Mechanical and microstructure comparison between microwave and spark plasma sintering of Al–B<sub>4</sub>C composite, *J. Alloy Cmpds* 655 (2016) 93–98.
- [24] E. Ghasali, A. Pakseresht, F.S. Kooshail, M. Agheli, T. Ebadzadeh, Investigation on microstructure and mechanical behaviour of Al–ZrB<sub>2</sub> composite prepared by microwave and spark plasma sintering, *Mater. Sci. Eng. A* 627 (2015) 27–30.
- [25] M. Gupta, W.L.E. Wong, Enhancing overall mechanical performance of metallic materials using two-directional microwave assisted rapid sintering, *Scr. Mater.* 52 (2005) 479–483.
- [26] M.H. Lee, J.H. Kim, J.S. Park, Fabrication of Ni–Nb–Ta metallic glass reinforced Al-based alloy matrix composites by infiltration casting process, *Scr. Mater.* 50 (11) (2004) 1367–1371.
- [27] J.Y. Kim, S. Scudino, U. Kuhn, B.S. Kim, Production and characterization of brass-matrix composites reinforced with Ni<sub>59</sub>Zr<sub>20</sub>Ti<sub>16</sub>Si<sub>2</sub>Sn<sub>5</sub> glassy particles, *Metals* 2 (2) (2012) 79–94.
- [28] S. Sankaranarayanan, V.H. Shankar, S. Jayalakhshmi, N.Q. Baua, M. Gupta, Development of high performance magnesium composites using Ni<sub>50</sub>Ti<sub>50</sub> metallic glass reinforcement and microwave sintering approach, *J. Alloy Cmpds* 627 (2015) 192–199.
- [29] D.R. Ni, J.J. Wang, Z.N. Zhou, Z.Y. Ma, Fabrication and mechanical properties of bulk NiTi/Al composites prepared by friction stir processing, *J. Alloy Cmpds* 586 (2014) 368–374.